J. Math. Biology (1984) 20: 133–152

Journal of
Mathematical
Biology

1:1 and 2:1 phase entrainment in a system of two coupled limit cycle oscillators

W. L. Keith and R. H. Rand

Department of Theoretical and Applied Mechanics, Cornell University, Ithaca, NY 14853, USA

Abstract. A model of a pair of coupled limit cycle oscillators is presented in order to investigate the extent of, and the transition between, 1:1 and 2:1 phase entrainment, a phenomenon exhibited by numerous diverse biological systems. The mathematical form of the model involves a flow on a phase torus given by two coupled first order nonlinear ordinary differential equations which govern the oscillators' phase angles (i.e. their respective positions around their limit cycles). The regions corresponding to 1:1 and 2:1 phase entrainment in an appropriate parameter space are determined analytically and numerically. The bifurcations occurring during the transition from 1:1 to 2:1 phase entrainment are discussed.

Key words: Oscillators — limit cycles — phase entrainment — bifurcations

Introduction

Recent research on problems in bio-oscillation theory have utilized simplified models of limit cycle oscillators (Cohen et al. [1], Guevara and Glass [7], Ermentrout and Kopell [2], Hoppensteadt and Keener [8], Rand et al. [12]). In this paper we extend previous work by proposing a model of two limit cycle oscillators which takes into account both 1:1 and 2:1 phase entrainment.

We briefly cite the following examples of biological systems which have exhibited 2:1 phase entrainment:

In the vertebrate heart disorder known as cardiac arrhythmias, every other pulse generated by the sinuatrial node pacemaker is ineffective in driving the ventricular rhythm. The process by which a normal heart becomes diseased may be viewed as a transition from 1:1 to 2:1 phase entrainment (Guevara and Glass [7]).

In experiments on the neurobiology of swimming in the fish Icthyomyzon unicuspis (the lamprey), Cohen et al. [1] reported a transition between 1:1 and 2:1 phase entrainment as follows: An isolated spinal cord undergoing phase locked "fictive swimming" was lesioned, resulting in the observation that the two

portions of the cord on either side of the lesion became 2:1 phase entrained (whereas before the lesion the two portions were 1:1 phase entrained).

In this paper we shall be interested in certain aspects of the general problem of 1:1 versus 2:1 phase entrainment in a system of two oscillators. In particular we wish to address the question of the extent of 1:1 versus 2:1 entrainment as a function of the uncoupled frequencies and the coupling between the oscillators. In addition we shall discuss the nature of the transition between these two entrained states, and will show that in our model a complicated sequence of bifurcations accompanies this transition.

Model

We follow Cohen et al. [1] and postulate a general biological oscillator which exhibits a unique stable limit cycle oscillation. Since we wish to make the model as general as possible, we make no assumptions about the containing space, except that the number of dimensions (and hence the number of physical variables needed to describe the system) be greater than one. In order to describe the oscillation mathematically, we parameterize the limit cycle by its phase θ chosen to run from 0 to 2π radians over the course of a complete cycle. Moreover we assume that the phase $\theta(t)$ flows uniformly in time t:

$$\dot{\theta} = \omega \quad \text{implies } \theta(t) = \omega t + \theta(0) \pmod{2\pi}. \tag{1}$$

Here mod 2π means that we do not distinguish between values of θ which differ by multiples of 2π (since the limit cycle is topologically a circle).

In order to model the interaction between two such oscillators, we assume that the limit cycle in an individual oscillator continues to persist when perturbed by feedback from another oscillator (i.e. we assume that the limit cycle is structurally stable). If θ_1 and θ_2 represent the respective phases of the two oscillators, we write:

$$\dot{\theta}_1 = \omega_1 + h_1(\theta_1, \theta_2) \tag{2}$$

$$\dot{\theta}_2 = \omega_2 + h_2(\theta_1, \theta_2) \tag{3}$$

where $h_1(\theta_1, \theta_2)$ represents the influence of oscillator 2 on oscillator 1, and similarly for $h_2(\theta_1, \theta_2)$. Since each θ_i is defined mod 2π, we further assume that the functions $h_i(\theta_1, \theta_2)$ are 2π periodic in their arguments. We may envision the resulting flow as taking place on a two dimensional torus which may be represented as a square with opposite sides identified (see Fig. 1).

In Cohen et al. the functions h_i were chosen thus:

$$\dot{\theta}_1 = \omega_1 - \alpha \sin(\theta_1 - \theta_2) \tag{4}$$

$$\dot{\theta}_2 = \omega_2 + \alpha \sin(\theta_1 - \theta_2) \tag{5}$$

where α is a coupling coefficient. By subtracting these equations it is easy to show that if $|\omega_1 - \omega_2| < |2\alpha|$ this system exhibits two 1:1 phase locked motions, one stable and one unstable:

$$\theta_1(t) - \theta_2(t) = \arcsin\left(\frac{\omega_1 - \omega_2}{2\alpha}\right). \tag{6}$$

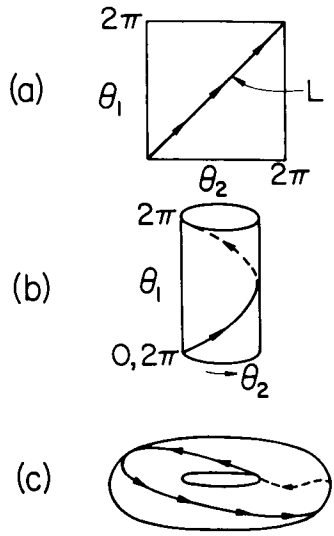

Fig. 1. The θ_1, θ_2 phase torus (c) can be represented by a square with opposite sides identified, as in (a). Fig. 1(b) shows the intermediate step in which the left and right sides of (a) have been joined, giving a cylinder. Fig. 1(c) results from joining the top and bottom ends of (b). The curve L represents a possible limit cycle

These motions represent limit cycles on the phase torus, see Fig. 2. Note that when plotted on a square with identified sides as in Fig. 2, these phase locked motions consist of straight line segments with slope unity. Note also that these limit cycles on the phase torus in the coupled system are distinct from and should not be confused with, the limit cycles in the space of physical variables in the dynamics of the original oscillators which were parameterized by θ_1 and θ_2.

In the case that $|\omega_1 - \omega_2| > |2\alpha|$, no such 1:1 phase locked limit cycles exist, and the motion is said to "drift".

In order to model 2:1 phase locking, we modify Eqs. (4), (5) as follows:

$$\dot{\theta}_1 = \omega_1 - \beta \sin(\theta_1 - 2\theta_2) \tag{7}$$

$$\dot{\theta}_2 = \omega_2 + \beta \sin(\theta_1 - 2\theta_2). \tag{8}$$

Here β is a coupling coefficient. In the case that $|\omega_1 - 2\omega_2| < |2\beta|$, this system exhibits two 2:1 phase locked motions, one stable and one unstable:

$$\theta_1(t) - 2\theta_2(t) = \arcsin\left(\frac{\omega_1 - 2\omega_2}{2\beta}\right). \tag{9}$$

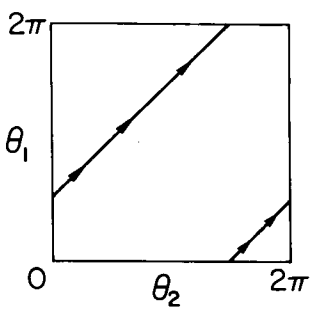

Fig. 2. A 1:1 phase locked motion. For clarity, only one of the two solutions in Eq. (6) has been shown

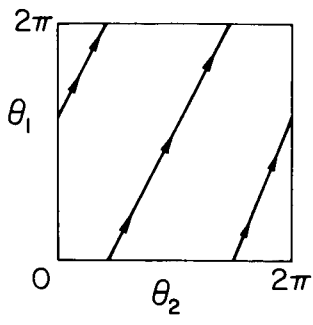

Fig. 3. A 2:1 phase locked motion. For clarity, only one of the two solutions in Eq. (9) has been shown

See Fig. 3. In the case that $|\omega_1 - 2\omega_2| > |2\beta|$, Eqs. (7), (8) do not admit 2:1 phase locked limit cycle solutions, but rather exhibit drift.

In Appendix E both sets of Eqs. (4), (5) and (7), (8) are derived from a perturbation method applied to two coupled van der Pol oscillators.

In order to obtain a model which exhibits both 1:1 and 2:1 phase locked motions, we combine the systems previously discussed in the following form:

$$\dot{\theta}_1 = \omega_1 - \alpha \sin(\theta_1 - \theta_2) - \beta \sin(\theta_1 - 2\theta_2) \tag{10}$$

$$\dot{\theta}_2 = \omega_2 + \alpha \sin(\theta_1 - \theta_2) + \beta \sin(\theta_1 - 2\theta_2). \tag{11}$$

For the special cases $\beta = 0$ and $\alpha = 0$, Eqs. (10), (11) reduce to Eqs. (4), (5) and (7), (8) respectively. Although these limiting cases can be derived from coupled van der Pol oscillators (see Appendix E), we propose the present model of coupled oscillators as independent of any derivation based on van der Pol oscillators, but rather as being of interest in its own right without a more elementary derivation. In a similar spirit, Hoppensteadt and Keener [8] presented a study of phase locking in radial isochron clocks based on the system:

$$\dot{\theta}_1 = 1$$

$$\dot{\theta}_2 = \omega + \varepsilon \sum_{m,n=-\infty}^{\infty} a_{m,n} \sin(m\theta_1 - n\theta_2)$$

(with $a_{m,n} = a_{n,m}$, $\forall m \neq n$).

Note the similarity in the coupling term between their model and our posited Eqs. (10), (11).

In order to reduce the number of parameters involved in this study, we set $\beta = 1 - \alpha$ in what follows:

$$\dot{\theta}_1 = \omega_1 - \alpha \sin(\theta_1 - \theta_2) - (1 - \alpha) \sin(\theta_1 - 2\theta_2) \tag{12}$$

$$\dot{\theta}_2 = \omega_2 + \alpha \sin(\theta_1 - \theta_2) + (1 - \alpha) \sin(\theta_1 - 2\theta_2). \tag{13}$$

We shall be interested in the dynamics of Eqs. (12), (13) as α is tuned from 0 to 1 for various values of ω_1 and ω_2. In particular we wish to investigate for which values of α the system behaves in a 1:1 or 2:1 manner.

Before proceeding with the analysis of this model, we wish to distinguish between the kind of 1:1 (or 2:1) behavior exhibited by Eqs. (12), (13) in the case that $\alpha = 1$ (or $\alpha = 0$), called phase locking, and a more general kind of

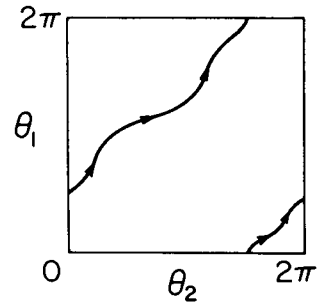

Fig. 4. A 1:1 phase entrained motion

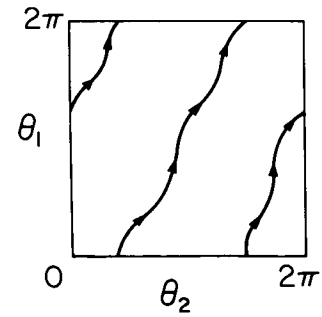

Fig. 5. A 2:1 phase entrained motion

interaction called phase entrainment. While a 1:1 phase locked motion involves a linear relationship between θ_1 and θ_2 (Eq. (6)), and plots as a straight line (Fig. 2), a 1:1 phase entrained motion will be defined to be a periodic motion for which θ_1 advances by 2π whenever θ_2 advances by 2π. That is, a motion will be said to be 1:1 phase entrained if

$$\theta_1|_{\theta_2=\theta^*} - \theta_1|_{\theta_2=\theta^*+2\pi} = 2\pi$$

for all θ^*. A 1:1 phase entrained motion is shown in Fig. 4. Note that 1:1 phase locked motions are special cases of 1:1 phase entrained motions in which a linear relationship exists between θ_1 and θ_2 for all time.

Similarly we define a 2:1 phase entrained motion to be one for which

$$\theta_1|_{\theta_2=\theta^*} - \theta_1|_{\theta_2=\theta^*+2\pi} = 4\pi$$

for all θ^*. That is, θ_1 advances by 4π whenever θ_2 advances 2π. See Fig. 5.

The importance of phase entrained motions lies in the fact that Eqs. (12), (13) admit 1:1 and 2:1 phase entrained motions for a wide range of parameter values, while these equations only exhibit 1:1 or 2:1 phase locked motions for $\alpha = 1$ or 0, respectively.

Analysis of the model

In the previous section we showed that the two oscillator model given by Eqs. (12), (13) exhibits 1:1 and 2:1 phase locking when $\alpha = 1$ and 0 respectively. In Appendix A we show that this model also exhibits a 3:2 phase locked motion

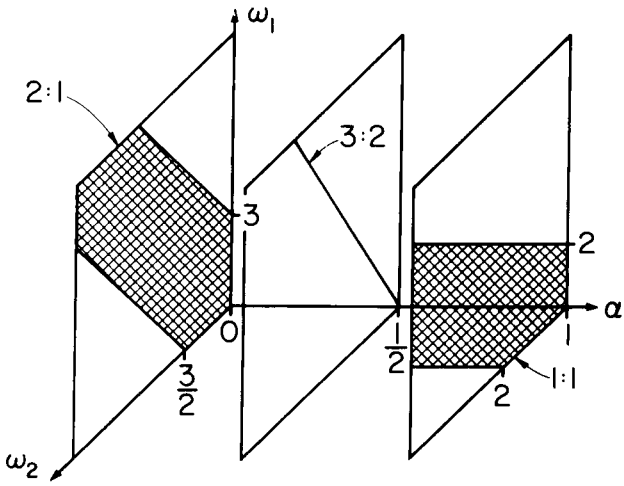

Fig. 6. Phase locked regions in ω_1, ω_2, α parameter space. The planes $\alpha = 0, 1$ contain regions of 2:1 and 1:1 locking, respectively, shown shaded. The plane $\alpha = \frac{1}{2}$ contains the indicated line on which 3:2 locking occurs

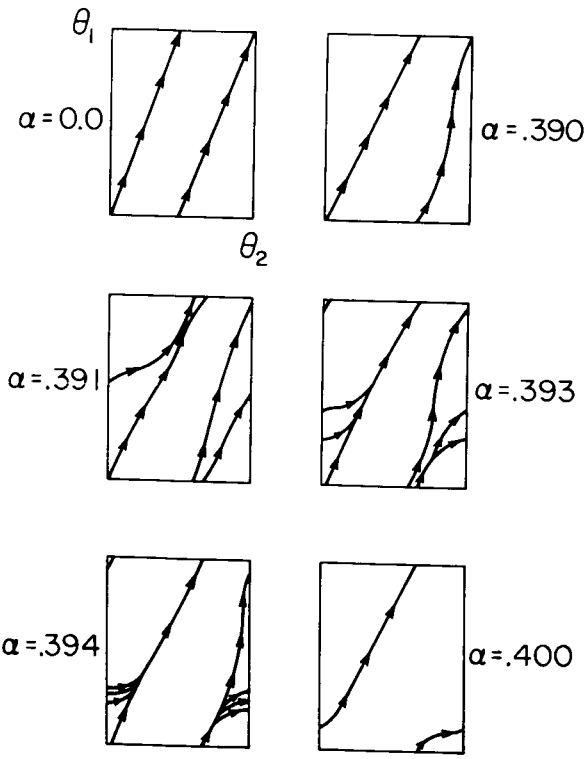

Fig. 7. Flow on the θ_1, θ_2 phase torus during transition from 2:1 to 1:1 phase entrained motions. As α increases from 0.39 to 0.4, a complicated sequence of bifurcations occurs which is conjectured to involve p:q phase entrained motions for all rational p/q between 1 and 2. Here, we display the 2:1, 3:2, 4:3, 5:4, and 1:1 cases. Note that when $\alpha = 0$ we have a 2:1 phase *locked* motion

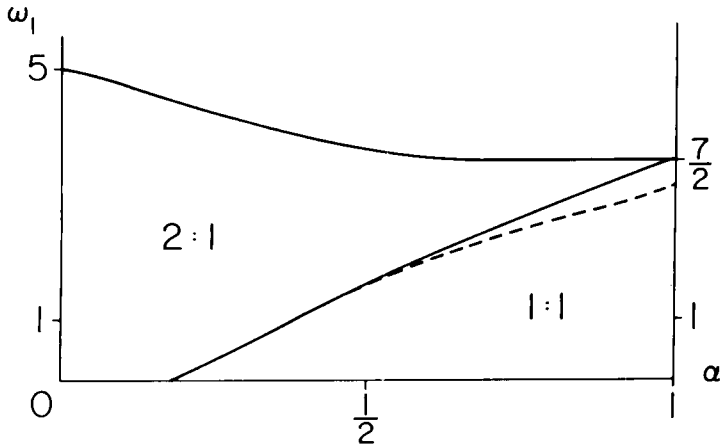

Fig. 8. 1:1 and 2:1 phase entrainment regions in ω_1, α space with $\omega_2 = 1$. The dashed line represents the boundary of the 1:1 region and intersects the line $\alpha = 1$ at $\omega_1 = 3$ (see Appendix A)

when $\alpha = \frac{1}{2}$, and that no other phase locked motions are possible. See Fig. 6 where the regions of phase locking are displayed in ω_1, ω_2, α parameter space.

We pass now from consideration of phase locked motions to phase entrained motions. To reduce the number of parameters, we set $\omega_2 = 1$ in all that follows.

We begin by presenting the results from typical numerical integrations of Eqs. (12), (13). We set $\omega_1 = \omega_2 = 1$ and vary α from 0 to 1. For $0 < \alpha \lesssim 0.39$, the system displays 2:1 phase entrainment, while for $0.40 \lesssim \alpha < 1$, 1:1 phase entrainment is observed. A complicated sequence of bifurcations occurs in the transition region, $0.39 \lesssim \alpha \lesssim 0.40$, see Fig. 7. We will return to a discussion of these bifurcations later.

Since the attraction onto a stable limit cycle becomes very weak as α approaches a critical (bifurcation) value, the numerical integrations must be carried out over very long time intervals. In order to avoid this difficulty, we developed an analytical-numerical technique which more efficiently yields the critical value of α at which a $p:q$ phase entrained solution ceases to exist. The details of this method are given in Appendix B. The resulting 1:1 and 2:1 entrainment regions in the ω_1, α plane are shown in Fig. 8. When $\alpha = 0$ and 1, the transition curves for 2:1 and 1:1 entrainment respectively yield the critical value of ω_1 obtained from the previous phase locked analysis.

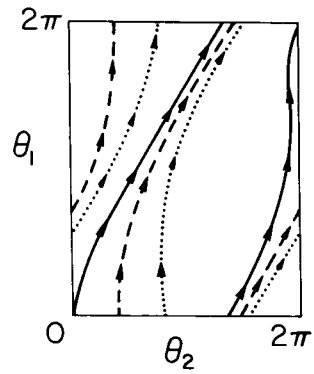

Fig. 9. A 2:1 drift flow (3 distinct trajectories are shown)

In particular, for $\alpha = 1$, the 2:1 entrainment transition curves intersect at $\omega_1 = \frac{7}{2}$, forming a wedge shaped region (Fig. 8). The point $\omega_1 = \frac{7}{2}$, $\alpha = 1$ may be analytically shown to correspond to a 2:1 drift solution (Keith [9]). (By a 2:1 drift solution we mean a situation in which the phase torus is filled with 2:1 phase entrained motions, none of which are attracting, see Fig. 9.)

We supplemented this numerical work in the neighborhood of this wedge-shaped region with a perturbation method. At the point $\omega_1 = \frac{7}{2}$, $\alpha = 1$, an exact solution of the 2:1 drifting motion is known (Cohen et al. [1]). We set $\varepsilon = 1 - \alpha$ and $\omega_1 = \frac{7}{2} + \lambda\varepsilon + O(\varepsilon^2)$, and perturbed off the exact solution for small ε. We offer a brief summary of the method in Appendix C, and here note just that the resulting values of slope λ turn out to be $0, -3$. The resulting wedge shaped region agrees closely with the previous numerical results, Fig. 10.

Next we offer a proof of the existence of 1:1 and 2:1 phase entrained motions based on the Poincare–Bendixson theorem. The exact nature of this proof complements the approximate nature of the previous numerical and perturbation results. Appendix D contains a summary of this work, which results in the regions of 1:1 and 2:1 phase entrainment shown in Fig. 11. Note that the method involves

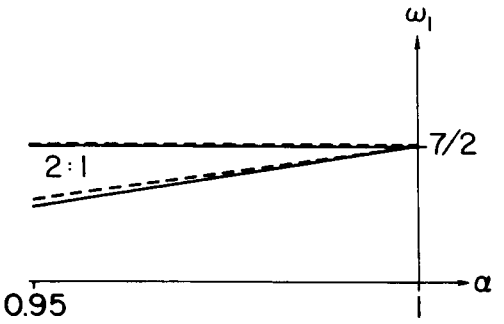

Fig. 10. The wedge shaped region of 2:1 phase entrainment near $\alpha = 1$. The dotted lines are the results from perturbation theory. The solid lines are the results from the numerical integration of the F equation

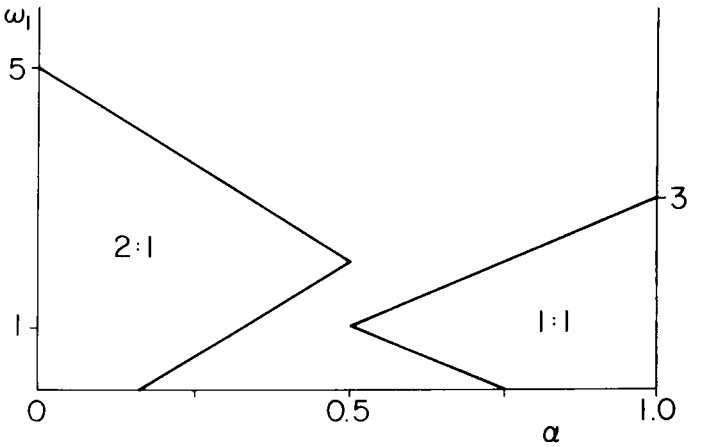

Fig. 11. The regions in the ω_1, α plane (with $\omega_2 = 1$) in which the existence of limit cycles (corresponding to 1:1 and 2:1 phase entrained motions) may be proven from the Poincare–Bendixson theorem. See Appendix D. The boundaries of the displayed regions are obtained analytically, and found to be straight line segments

only sufficient conditions on the existence of phase entrained motions, so the associated regions in Fig. 11 lie inside the corresponding numerically obtained regions shown in Fig. 8.

Let us now consider the nature of the bifurcations which occur during the transition from 1:1 to 2:1 phase entrainment. The analytical-numerical technique discussed in Appendix B and utilized to obtain the limiting parameter values for 1:1 and 2:1 entrainment in Fig. 8, was used again here. For a given ratio p/q, a differential equation was derived (see Appendix B) which exhibits periodic solutions only for those parameter values for which there is p: q phase entrainment. We numerically integrated this equation for nine different ratios p/q between 1 and 2, fixing $\omega_1 = \omega_2 = 1$ and varying α (cf. Fig. 7). The results are shown in Fig. 12. Each value of p/q corresponds to a plateau of phase entrainment, the size of the plateau being larger, the smaller the value of q is. Since this flow on the torus T^2 has no singular points, a Poincare map on a cross section can be

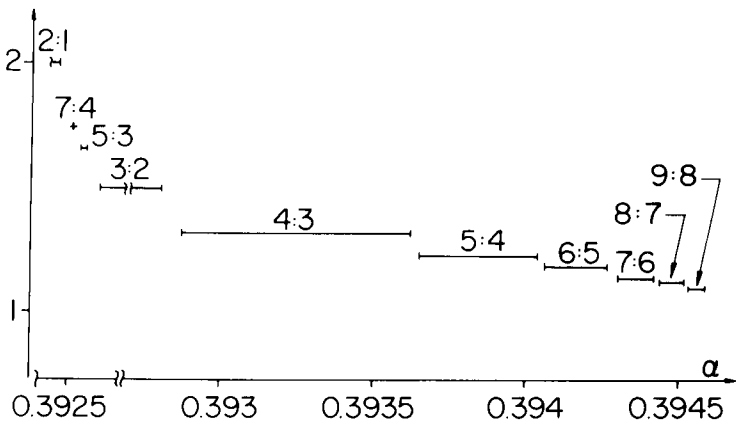

Fig. 12. Plateaus of p: q phase entrainment in the α, p/q plane. (Note the breaks in the horizontal scale)

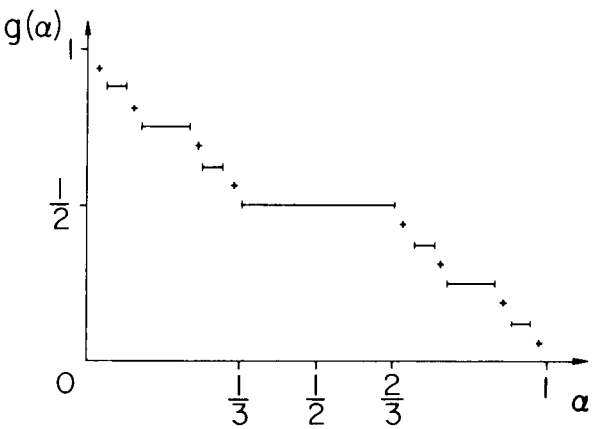

Fig. 13. The Cantor function $g(\alpha)$ with 15 intervals shown

constructed. This map will be a diffeomorphism on S^1, and therefore one can apply the results of Denjoy [4] (cf. Guckenheimer and Holmes [6]) which show that the rotation number depends continuously on parameters (here α and ω_1). We conclude that all rational p/q between 1 and 2 are exhibited by this system. We also expect generically to find frequency plateaus for all rational rotation numbers. An example of function which exhibits this behavior is provided by the Cantor function, defined as follows:

We consider the closed interval $0 \leq \alpha \leq 1$. For $\frac{1}{3} < \alpha < \frac{2}{3}$ we set $g(\alpha) = \frac{1}{2}$, for $\frac{1}{3^2} < \alpha < \frac{2}{3^2}$ and $\frac{7}{3^2} < \alpha < \frac{8}{3^2}$ we set $g(\alpha) = \frac{1}{4}$ and $\frac{3}{4}$ respectively, and so forth. At the nth step, the function $g(\alpha)$ is given values over the 2^{n-1} open intervals of length $(\frac{1}{3})^n$ midway between the values of $g(\alpha)$ on the neighboring 2^{n-2} intervals of length $(\frac{1}{3})^{n-1}$. In the limit as $n \to \infty$, we have a continuous function $g(\alpha)$, whose slope is zero almost everywhere. The Cantor function $g(\alpha)$ is shown in Fig. 13 with 15 intervals plotted.

Summary and conclusions

A system of two coupled first order nonlinear ordinary differential equations has been proposed to govern the behavior of 2 generalized biological oscillators. Each uncoupled oscillator is assumed to exhibit a limit cycle which persists after coupling and which is modeled by its phase $\theta_i(t)$.

The system exhibits "phase-locked" motions, for which (in the 1:1 case, for example) the difference $\theta_1(t) - \theta_2(t)$ is constant, as well as "phase entrained" motions, for which (again in the 1:1 case) $\theta_1(t) - \theta_2(t)$ varies periodically. Although phase-locked motions represent very special behavior in the model, phase entrained motions (1:1 and 2:1) occur in a large region of parameter space.

In the neighborhood of $\alpha = 1$, where the 1:1 coupling term predominates, the 1:1 phase-entrainment region is centered around a natural frequency ratio of $\omega_1/\omega_2 = 1$. Similarly, in the neighborhood of $\alpha = 0$, where the 2:1 coupling term predominates, the 2:1 phase-entrainment region is centered around a frequency ratio of $\omega_1/\omega_2 = 2$. See Fig. 8.

For a given value of ω_1, the two regions are separated by a narrow band which becomes vanishingly small as $\omega_1 \to 0$. See Fig. 8. Across this band, all rational $p:q$ phase-entrained motions are conjectured to occur, for $1 < p/q < 2$. For $\omega_1 = \frac{7}{2}$, a wedge-shaped region of 2:1 phase-entrainment occurs around $\alpha = 1$. See Fig. 8.

Figure 8 illustrates that a change in magnitude of the coupling α, or of the natural frequency ω_1 (or more generally of the frequency ratio ω_1/ω_2) can lead to a transition from 1:1 to 2:1 phase-entrainment. This result is of particular significance in modeling a pathological condition occurring in cardiac pacemakers known as 2:1 AV block (Glass and Mackey, [5]).

During normal pacemaker activity, an action potential initiated at the sinoatrial (SA) node causes atrial contraction and also excites the atrioventricular (AV) node. Excitation of the AV node initiates the release of a second action potential, causing ventricular contraction a short time after the atrial contraction. During 2:1 AV block, the SA node loses its role as pacemaker, such that every other generated pulse is ineffective in driving the ventricular rhythm.

The SA node and AV node have been modeled as two coupled oscillators as early as 1928 by van der Pol and van der Mark [13], and more recently by Guevara and Glass [7]. (Note, however, that these previous models are mathematically very different from the approach taken in this paper.) Using our model, the onset of 2:1 AV block could be explained as being caused either by a change in frequency ratio or in coupling coefficient leading to transition from 1:1 to 2:1 phase entrainment.

Although the model presented in this work offers a very simplified picture of the dynamics of a two oscillator system, it is hoped that it will be useful to biologists in thinking about the qualitative behavior associated with 1:1 and 2:1 entrainment.

Acknowledgments. The authors wish to thank Philip Holmes for numerous contributions to this work. This work was partially supported by Air Force Grant #AFOSR-84-0051.

Appendix A. Phase locked motions

In this section we show that Eqs. (12), (13) exhibit 1:1, 2:1, and 3:2 phase locked motions, and no others.

For $p:q$ phase locking we require that

$$\theta_1(t) = \frac{p}{q}\theta_2(t) + \theta_{10} \quad \text{for all } t, \tag{A1}$$

where p and q are relatively prime (that is, are integers with no common factor besides unity), and where we take without loss of generality $\theta_2(0) = 0$, $\theta_1(0) = \theta_{10}$.

Differentiating (A1) with respect to time, we obtain the condition

$$q\dot{\theta}_1 = p\dot{\theta}_2. \tag{A2}$$

Substituting Eqs. (12), (13) into (A2), we find

$$q(\omega_1 - \alpha \sin(\theta_1 - \theta_2) - (1-\alpha)\sin(\theta_1 - 2\theta_2)) = p(\omega_2 + \alpha \sin(\theta_1 - \theta_2) + (1-\alpha)\sin(\theta_1 - 2\theta_2)). \tag{A3}$$

Using (A1) this may be written

$$\alpha \sin(A\theta_2(t) + \theta_{10}) + (1-\alpha)\sin(B\theta_2(t) + \theta_{10}) + C = 0 \tag{A4}$$

where

$$A = \frac{p}{q} - 1, \qquad B = \frac{p}{q} - 2, \qquad C = \omega_2\left(\frac{p}{q} - \frac{\omega_1}{\omega_2}\right)\Big/\left(\frac{p}{q} + 1\right).$$

Now Eq. (A4) is of the general form

$$k_1 \sin f(t) + k_2 \sin g(t) + k_3 = 0 \tag{A5}$$

where

$$k_1 = \alpha, \quad k_2 = 1 - \alpha, \quad k_3 = C, \quad f(t) = A\theta_2(t) + \theta_{10}, \quad g(t) = B\theta_2(t) + \theta_{10}.$$

In order for (A5) to be satisfied on an open interval in t, in the general case in which the functions $f(t)$, $g(t)$ and the constant function 1 are linearly independent, we require that

$$k_1 = k_2 = k_3 = 0. \tag{A6}$$

If, however, $f(t) \equiv \pm g(t) \not\equiv$ constant, then (A5) is satisfied by

$$k_1 \pm k_2 = 0, \qquad k_3 = 0. \tag{A7}$$

On the other hand, if $f(t) \equiv$ constant, while $g(t) \not\equiv$ constant, then (A5) gives

$$k_1 \sin f + k_3 = 0, \qquad k_2 = 0. \tag{A8}$$

If $g(t) \equiv$ constant, while $f(t) \not\equiv$ constant, then (A5) gives

$$k_2 \sin g + k_3 = 0, \qquad k_1 = 0. \tag{A9}$$

Finally, if both $f(t)$ and $g(t)$ are constants, then (A5) simply becomes

$$k_1 \sin f + k_2 \sin g + k_3 = 0. \tag{A10}$$

Thus (A4) may possibly be satisfied in one of the 5 ways (A6)–(A10). However, it may be seen immediately that (A6) and (A10) are impossible. Equation (A7) requires either $f(t) \equiv g(t)$ or $f(t) \equiv -g(t)$. The former condition requires that $A = B$, which is impossible, while the latter condition requires $A = -B$ and $\theta_{10} = 0$. The condition $A = -B$ is satisfied by taking $p/q = \frac{3}{2}$, in which case (A7) requires that $k_1 - k_2 = 0$, i.e. $\alpha = \frac{1}{2}$, as well as $k_3 = C = 0$, i.e. $\omega_2/\omega_1 = \frac{3}{2}$. Thus we find that when $\alpha = \frac{1}{2}$ and $\omega_2/\omega_1 = \frac{3}{2}$, a 3:2 phase locked motion exists.

Returning to conditions (A6)–(A10), we find that (A8) is satisfied if $f(t) \equiv$ constant, i.e. if $A = 0$ which requires that $p = q = 1$, in which case (A8) gives

$$\alpha \sin \theta_{10} + \frac{\omega_1 - \omega_2}{2} = 0 \quad \text{and} \quad \alpha = 1$$

i.e.

$$\sin \theta_{10} = \frac{\omega_2 - \omega_1}{2}$$

which requires $|\omega_1 - \omega_2| \leq 2$. Thus when $\alpha = 1$, a 1:1 phase locked motion exists only if $|\omega_2 - \omega_1| \leq 2$.

Similarly, (A9) requires $g(t) \equiv$ constant, i.e. $B = 0$ which requires $p = 2q$, in which case (A9) gives

$$(1 - \alpha) \sin \theta_{10} + \frac{2\omega_1 - \omega_2}{3} = 0 \quad \text{and} \quad \alpha = 0$$

i.e.

$$\sin \theta_{10} = \frac{\omega_2 - 2\omega_1}{3}$$

which requires $|\omega_2 - 2\omega_1| \leq 3$. Thus when $\alpha = 0$, a 2:1 phase locked motion exists only if $|\omega_2 - 2\omega_1| \leq 3$.

Appendix B. Derivation of the F equation

In this section we develop an analytical-numerical method in order to find the regions of $p:q$ phase entrainment more efficiently than by simply numerically integrating Eqs. (12), (13). We derive an equation, Eq. (B6) below, which exhibits periodic solutions if and only if Eqs. (12), (13) exhibit $p:q$ phase entrainment. Setting $\omega_2 = 1$ and adding Eqs. (12) and (13) gives

$$\dot{\theta}_1 + \dot{\theta}_2 = \omega_1 + 1. \tag{B1}$$

Integrating (B1) with respect to time we obtain

$$\theta_1(t) + \theta_2(t) = (\omega_1 + 1)t + \theta_1(0) + \theta_2(0). \tag{B2}$$

Equation (B1) may be satisfied by solutions of the form

$$\theta_1(t) = \left(\frac{2\pi p}{T}\right)t + F(t) \equiv r_1 t + F(t), \qquad r_1 = \frac{2\pi p}{T} \tag{B3}$$

$$\theta_2(t) = \left(\frac{2\pi q}{T}\right)t - F(t) \equiv r_2 t - F(t), \qquad r_2 = \frac{2\pi q}{T} \tag{B4}$$

where $t_0 = 0$ and $\theta_1(0) = -\theta_2(0) = F(0)$. Adding (B3) and (B4) and comparing the result to (B2) we observe

$$r_1 + r_2 = \omega_1 + 1. \tag{B5}$$

Substituting (B3) and (B4) into (12) we obtain

$$\dot{F} = \omega_1 - r_1 + \alpha \sin((r_2 - r_1)t - 2F) + (1-\alpha)\sin((2r_2 - r_1)t - 3F) \tag{B6}$$

which is a first-order, nonautonomous, nonlinear differential equation for $F(t)$. From (B3) and (B4) we have

$$\Delta(q\theta_1 - p\theta_2)|_{t=T} = (q+p)\Delta F(t)|_{t=T}. \tag{B7}$$

For p: q phase entrainment to exist at time $t = T$, we require $\Delta F(t)|_{t=T} = 0$. This implies that a periodic solution must exist for $F(t)$. Equation (B6) must then yield a periodic solution for $F(t)$, where the period is governed by the p and q of interest, which determine r_1 and r_2.

For $p = 2$ and $q = 1$, we obtain

$$r_1 = 2r_2. \tag{B8}$$

Combining (B5) and (B8) we obtain

$$r_1 = \tfrac{2}{3}(\omega_1 + 1) \tag{B9}$$

and

$$r_2 = \frac{\omega_1 + 1}{3}. \tag{B10}$$

Substituting (B10) and (B9) into (B6) gives

$$\dot{F} = \frac{\omega_1 - 2}{3} - \alpha \sin\left(\left(\frac{\omega_1 + 1}{3}\right)t + 2F\right) - (1-\alpha)\sin 3F. \tag{B11}$$

Values of ω_1 and α for which periodic solutions of period $6\pi/(\omega_1 + 1)$ exist for Eq. (B11) correspond to regions of 2:1 phase entrainment in the ω_1, α plane. Equation (B11) was integrated numerically. For a fixed value of ω_1, α was varied until loss of periodicity occurred at or before 5 periods. For 1:1 entrainment, an equation analogous to (B11) was derived and regions of 1:1 entrainment were similarly obtained by numerical integration.

Appendix C. Perturbation method

In this section, we present a perturbation method which serves to supplement information about the phase entrainment plot in the neighborhood of the point in parameter space where $\omega_1 = \frac{7}{2}$, $\omega_2 = 1$, and $\alpha = 1$. We approximate the upper and lower boundaries of the 2:1 phase entrainment region in the neighborhood of $\alpha = 1$ by straight lines which intersect at $\omega_1 = \frac{7}{2}$ and $\alpha = 1$ forming a wedge. In the neighborhood of the wedge,

$$\alpha = 1 - \varepsilon \tag{C1}$$

$$\omega_1 = \tfrac{7}{2} + \lambda\varepsilon + O(\varepsilon^2). \tag{C2}$$

When $\varepsilon = 0$, the exact solution to Eqs. (12) and (13) is known (Cohen et al. [1]). When ε is not identically zero, $\theta_1(t)$ and $\theta_2(t)$ will depend on ε. For 2:1 phase entrainment, at some time $t = t^*$, $\theta_1(t^*) = 4\pi$ and $\theta_2(t^*) = 2\pi + \theta_0$. Since t^* will depend on ε, it is convenient to stretch time such that $\tau = t(1 + U\varepsilon + O(\varepsilon^2))$, where U is an undetermined constant. We then transform the independent variable from t to τ and look for a solution to (12) and (13) of the form

$$\theta_1(\tau) = \theta_1^0(\tau) + \varepsilon\xi_1(\tau) \tag{C3}$$

$$\theta_2(\tau) = \theta_2^0(\tau) + \varepsilon\xi_2(\tau). \tag{C4}$$

We then substitute (C3) and (C4) into (12) and (13), expand the sine terms in a Taylor series, and neglect terms of $O(\varepsilon^2)$. Equating terms of $O(\varepsilon)$ we obtain

$$\xi_1' = -\frac{7U}{2} + (U+1)\sin(\theta_1^0 - \theta_2^0) + \lambda$$
$$-\cos(\theta_1^0 - \theta_2^0)(\xi_1 - \xi_2) - \sin(\theta_1^0 - 2\theta_2^0) \tag{C5}$$
$$\xi_2' = -U - (U+1)\sin(\theta_1^0 - \theta_2^0) + \sin(\theta_1^0 - 2\theta_2^0)$$
$$+\cos(\theta_1^0 - \theta_2^0)(\xi_1 - \xi_2). \tag{C6}$$

For 2:1 phase entrainment, it may be shown (Keith [9]) that

$$\tau^* = 4\pi/3 \tag{C7}$$
$$U = 2\lambda/9. \tag{C8}$$

Subtracting (C6) from (C5), using (C8), and defining $\eta = \xi_1 - \xi_2$, we obtain

$$\eta' + 2\eta\cos(\theta_1^0 - \theta_2^0) = 2(2\lambda/9 + (2\lambda/9 + 1)\sin(\theta_1^0 - \theta_2^0) - \sin(\theta_1^0 - 2\theta_2^0)). \tag{C9}$$

Equation (C9) is of the form

$$\frac{d\eta}{dt} + P(\tau)\eta = Q(\tau). \tag{C10}$$

This first-order linear o.d.e. has the solution

$$\eta(\tau) = e^{-\int_0^\tau P(\tau)\,d\tau}\int_0^\tau Q(\tau)\, e^{\int_0^\tau P(\tau)\,d\tau}\,d\tau + \hat{c}\, e^{-\int_0^\tau P(\tau)\,d\tau} \tag{C11}$$

where $\eta(0) = \xi_1(0) - \xi_2(0) = \hat{c}$. Without loss of generality we choose $\xi_1(0) = \xi_2(0)$, i.e. $\hat{c} = 0$. Equation (C11) evaluated at $\tau = \tau^* = 4\pi/3$ becomes

$$0 = \int_0^{4\pi/3} Q(\tau)\, e^{\int_0^\tau P(\tau)\,d\tau}\,d\tau \tag{C12}$$

which is of the form $H(\theta_0, \lambda) = 0$ where $\theta_0 = \theta_2(0)$. Equation (C12) may be shown to be 2π periodic in θ_0. Treating θ_0 as a variable and λ as a parameter, values of λ for which zeroes of $H(\theta_0, \lambda)$ exist correspond to the region of 2:1 phase entrainment in the $\omega_1 - \alpha$ plane. The limiting values of λ for which zeroes exist correspond to the boundaries of the 2:1 entrainment region. Equation (C12) was integrated numerically for $-4 \leq \lambda \leq 1$. The results of this analysis are shown in Fig. 10. The limiting values of λ are found to be approximately $\lambda = -3$ and $\lambda = 0$.

Appendix D. Poincaré–Bendixson theorem

In this section we offer a proof of the existence of the limit cycles in θ_1, θ_2 phase space. We begin by reviewing the theory of Poincaré's proofs of existence of limit cycles in the plane.

The Poincaré–Bendixson theorem for flow on a plane states that it is sufficient for the existence of at least one closed trajectory in a domain D that (Fig. D1)

a) Trajectories enter (or leave) D through every point on the bounding curves C_1 and C_2, and
b) There are no singular points in D or on C_1 or C_2.

Let the vector field in the x, y phase plane be given by

$$\mathbf{V} = \dot{x}\hat{i} + \dot{y}\hat{j}$$

where $\hat{i}$ and $\hat{j}$ are orthogonal unit vectors in the x and y directions respectively. If a curve C exists such that at no point on C is the vector field $\mathbf{V}$ zero or tangent to C, then C is called a curve without contact. For a continuous vector field $\mathbf{V}$, a curve with contacts cannot generally serve as a bounding curve C_1 or C_2 since the vector field along C enters D at some points and leaves at others, as shown in Fig. D2. An exception occurs when the contact is of higher order (Minorsky [14]).

For a "topographic family" consisting of closed curves given by $f(x, y) = k$, and a given vector field $\mathbf{V}$, let $k_1 < k < k_2$ correspond to members of this family which are curves with contacts, and

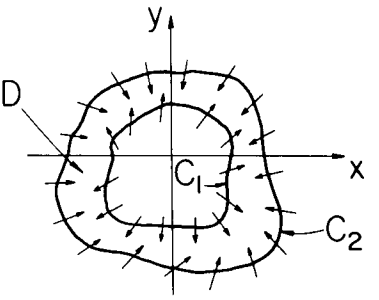

Fig. D1. The region D in which a stable limit cycle exists

$k < k_1$ and $k > k_2$ correspond to members without contacts. The locus of points at which contact exists forms a continuous curve which may or may not be closed. The case where such a curve is closed (and the topographic family consists of circles centered at the origin) is shown in Fig. D3. Poincare refers to this curve as the *curve of contacts.* When the curve of contacts is closed, the domain D defined by the topographic family for $k_1 < k < k_2$ contains a closed trajectory that is a limit cycle. The curves $f(x, y) = k_1$, and $f(x, y) = k_2$ serve as the bounding curves along which all trajectories enter or leave D. If all trajectories enter D, the limit cycle is stable, and if all trajectories leave D, the limit cycle is unstable. We now proceed to apply this theory to our system.

We showed that for p: q entrainment, a periodic solution of period T exists for the corresponding differential equation for $F(t)$. The phase space for this flow may be viewed as a cylinder whose circumference is the period T and whose axis is $F(t)$, as shown in Fig. D4. For this system we choose the topographic family to be $f(F, t) = F = \text{constant}$. We then proceed to find a range of parameter values over which a domain D such as that shown in Fig. D5 exists.

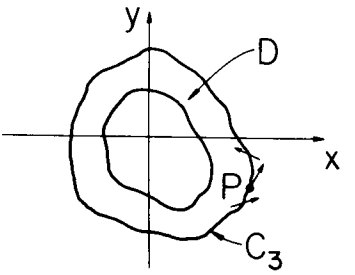

Fig. D2. C_3 is a curve with contact (since the vector field is tangent to C_3 at point P) which cannot serve as a bounding curve such as C_1 or C_2 in Fig. D1

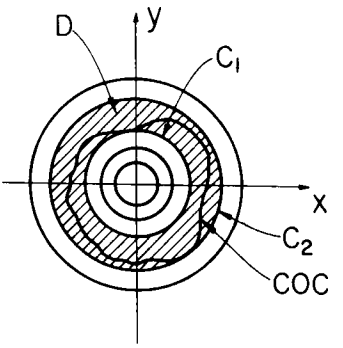

Fig. D3. COC is the curve of contacts, with the topographic system consisting of circles centered at the origin

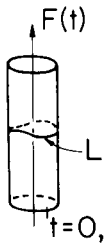

Fig. D4. The cylindrical phase space

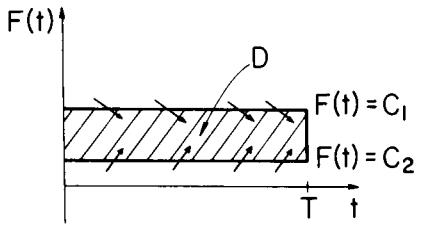

Fig. D5. The topographical system $F(t) = \text{constant}$

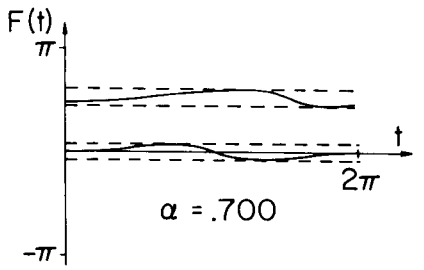

Fig. D6. The solids lines are curves of contacts. The dotted lines are members of the topographic family which serve as boundaries of the regions in which limit cycles exist. The region D_1 (D_2) lies between the upper (lower) pair of dotted lines. Here $\alpha = 0.7$ and $\omega_1 = 1$

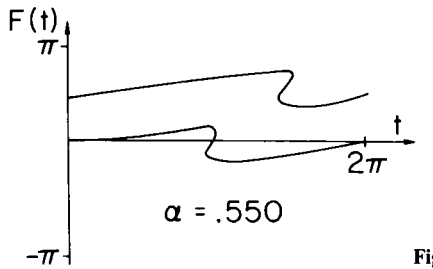

Fig. D7. The curves of contacts with $\alpha = 0.55$ and $\omega_1 = 1$

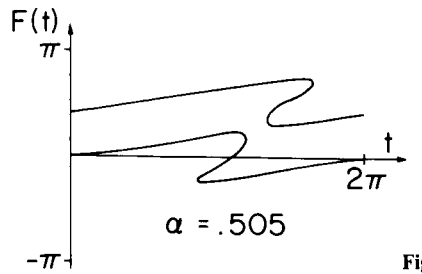

Fig. D8. The curves of contacts with $\alpha = 0.505$ and $\omega_1 = 1$

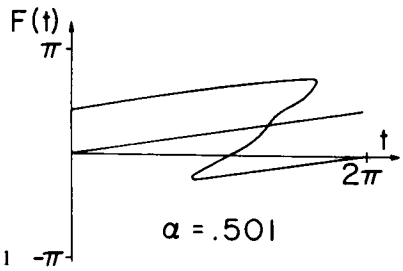

Fig. D9. The curves of contacts with $\alpha = 0.501$ and $\omega_1 = 1$

The vector field in the $F-t$ plane is given by

$$\mathbf{V} = \hat{i} + \dot{F}\hat{j}.$$

The normal to the topographic family $f(F, t) = F$ is given by

$$\nabla f(F, t) = f_t\hat{i} + f_F\hat{j} = \hat{j}.$$

Then for curves of contacts,

$$\nabla f \cdot \mathbf{V} = \dot{F} = 0.$$

From Eq. (B6) derived in Appendix B for $\dot{F}(t)$ we obtain the equation for the curve of contacts for 1:1 phase entrainment,

$$0 = \left(\frac{\omega_1 - 1}{2}\right) - \alpha \sin 2F + (1-\alpha)\sin\left(\left(\frac{\omega_1 + 1}{2}\right)t - 3F\right) \tag{D1}$$

and for 2:1 phase entrainment,

$$0 = \left(\frac{\omega_1 - 2}{3}\right) - \alpha \sin\left(\left(\frac{\omega_1 + 1}{3}\right)t + 2F\right) - (1-\alpha)\sin 3F \tag{D2}$$

where ω_2 has been set equal to 1, and ω_1 and α are retained as parameters. Figure D6 shows two of the curves of contacts given by Eq. (D1) as solid lines (where $\omega_1 = 1$ and $\alpha = 0.7$). The dotted lines are members of the topographic family which serve as the boundaries of the region in which the limit cycles exist. Here the region D_1 contains a stable limit cycle and D_2 contains an unstable limit cycle. It should be noted that in general the limit cycles (which are the periodic solutions for $F(t)$, and not shown in Fig. D6) do not coincide with the curves of contacts and may or may not touch the bounding curves of a region D.

As α is varied, the diagram corresponding to Fig. D6 (for $\alpha = 0.7$) changes, as shown, for example, in Figs. D7–D9 (for $\alpha = 0.55$, 0.505, and 0.501, respectively). While the previous argument for the existence of limit cycles applies to Figs. D7 and D8, it does not hold for Fig. D9, since the intersection of the two curves of contacts eliminates the associated regions D of Fig. D6. By analytically requiring the two curves of contacts to just touch, we obtain the boundaries for 1:1 and 2:1 phase entrainment shown in Fig. 11 (see Keith [9] for further details).

Appendix E. Coupled van der Pol oscillators

In this section we outline the derivation of Eqs. (4), (5) and (7), (8) from coupled van der Pol oscillators. We consider two van der Pol oscillators with weak coupling given by:

$$\ddot{\mathbf{u}} + \mathbf{W}\mathbf{u} - \varepsilon(\mathbf{I} - \mathbf{U}^2)\dot{\mathbf{u}} = \varepsilon\mathbf{g} \tag{E1}$$

where

$$\mathbf{u} = \begin{bmatrix} x_1 \\ x_2 \end{bmatrix}, \quad \mathbf{W} = \begin{bmatrix} \omega_1^2 & 0 \\ 0 & 1 \end{bmatrix}, \quad \mathbf{U} = \begin{bmatrix} x_1 & 0 \\ 0 & x_2 \end{bmatrix}, \quad \mathbf{g} = \begin{bmatrix} g_1 \\ g_2 \end{bmatrix}.$$

Here ω_2 has been taken to be unity without loss of generality. We take the coupling to be a general quadratic function of the velocities and displacements:

$$g_i = \sum_{j=1}^{2} \sum_{k=1}^{2} (a_{ijk} X_j X_k + c_{ijk} \dot{X}_j \dot{X}_k + b_{ijk} \dot{X}_j X_k + h_{ij} X_j + l_{ij} \dot{X}_j). \tag{E2}$$

This extends the study of Rand and Holmes [11], who took the g_i to be linear functions of X_j and $\dot{X}_j$. Using the two variable expansion perturbation method (cf. Cole [3]), the independent variable t is replaced by two new independent variables, ξ (stretched time) and η (slow time):

$$\xi = \Omega t, \qquad \Omega = 1 + \Omega_1 \varepsilon + O(\varepsilon^2), \qquad \eta = \varepsilon t.$$

Under this transformation, Eq. (E1) becomes

$$\mathbf{u}_{\xi\xi} + 2\varepsilon \mathbf{u}_{\xi\eta} + \mathbf{W}\mathbf{u} - \varepsilon(\mathbf{I} - \mathbf{U}^2)\mathbf{u}_{\xi} = \varepsilon \mathbf{g} \tag{E3}$$

where subscripts denote partial differentiation. Next we expand the dependent variables $X_1(\xi, \eta)$ and $X_2(\xi, \eta)$ in power series in ε:

$$X_i(\xi, \eta) = X_{i0}(\xi, \eta) + \varepsilon X_{i1}(\xi, \eta) + O(\varepsilon^2), \qquad i = 1, 2.$$

Substituting this expression into (E3) and equating coefficients of ε^0 we obtain:

$$X_{10} = A_1(\eta) \cos \omega_1 \xi + B_1(\eta) \sin \omega_1 \xi \tag{E4}$$

$$X_{20} = A_2(\eta) \cos \xi + B_2(\eta) \sin \xi. \tag{E5}$$

Equating the coefficients of ε^1 we obtain:

$$X_{11\xi\xi} + \omega_1^2 X_{11} = (1 - X_{10}^2) X_{10\xi} - 2X_{10\xi\eta} + g_1 \tag{E6}$$

$$X_{21\xi\xi} + X_{21} = (1 - X_{20}^2) X_{20\xi} - 2X_{20\xi\eta} + g_2. \tag{E7}$$

Equations (E4) and (E5) are substituted into (E6) and (E7), and the coefficients of the secular terms $\sin \omega_1 \xi$ and $\cos \omega_1 \xi$ in (E6) and $\sin \xi$ and $\cos \xi$ in (E7) are set equal to zero. Due to the large number of terms in g_1 and g_2, this calculation was performed using the symbolic manipulation program MACSYMA (cf. Rand [10]). We now have four differential equations for $A_1(\eta)$, $A_2(\eta)$, $B_1(\eta)$, and $B_2(\eta)$. We transform to polar coordinates such that

$$\begin{aligned} X_{10} &= R_1(\eta) \cos(\theta_1(\xi, \eta)) \\ X_{20} &= R_2(\eta) \cos(\theta_2(\xi, \eta)). \end{aligned} \tag{E8}$$

We wish to consider the 1 : 1 and 2 : 1 cases where $\omega_1 = 1$ and $\omega_1 = 2$ respectively. For the *1 : 1 case*, after manipulation (cf. Keith [9]) the differential equations for θ_1 and θ_2 become:

$$\frac{d\theta_1}{dt} = 1 - \frac{\varepsilon h_{11}}{2} + \frac{\varepsilon R_2}{2R_1}(h_{12} \cos(\theta_1 - \theta_2) - l_{12} \sin(\theta_1 - \theta_2)) \tag{E9}$$

$$\frac{d\theta_2}{dt} = 1 - \frac{\varepsilon h_{22}}{2} - \frac{\varepsilon R_1}{2R_2}(h_{21} \cos(\theta_1 - \theta_2) - l_{21} \sin(\theta_1 - \theta_2)). \tag{E10}$$

For the *2 : 1 case*, the differential equations for θ_1 and θ_2 become:

$$\frac{d\theta_1}{dt} = 2 - \frac{\varepsilon h_{11}}{4} - \frac{\varepsilon R_2^2}{8R_1}((a_{122} - c_{122}) \cos(\theta_1 - 2\theta_2) + b_{122} \sin(\theta_1 - 2\theta_2)) \tag{E11}$$

$$\begin{aligned} \frac{d\theta_2}{dt} = 1 - \frac{\varepsilon h_{22}}{2} - \varepsilon \frac{R_1}{4}((2(c_{212} + c_{221}) + (a_{212} + a_{221})) \cos(\theta_1 - 2\theta_2) \\ - (2b_{212} - b_{221}) \sin(\theta_1 - 2\theta_2)). \end{aligned} \tag{E12}$$

Note that R_1 and R_2 in Eqs. (E9) through (E12) also satisfy differential equations which we omit in our derivation of Eqs. (4), (5), (7), and (8).

For the *1:1 case*, we can obtain Eqs. (4) and (5) by making the following substitutions: Set $h_{12}=h_{21}=h_{11}=h_{22}=0$ and obtain:

$$\dot{\theta}_1 = 1-\varepsilon\left(\frac{R_2 l_{12}}{2R_1}\right)\sin(\theta_1-\theta_2) \tag{E13}$$

$$\dot{\theta}_2 = 1+\varepsilon\left(\frac{R_1 l_{21}}{2R_2}\right)\sin(\theta_1-\theta_2). \tag{E14}$$

The presence of ε in each of the coefficients of the sin terms restricts the phase coupling to be of $O(\varepsilon)$, which we expect since the van der Pol oscillators are weakly coupled. In the absence of coupling, each van der Pol oscillator moves on a limit cycle of radius 2. In the presence of weak coupling ($0<\varepsilon\ll 1$), the perturbed limit cycles may be assumed to be close to the unperturbed ones (cf. Rand and Holmes [11]), leading to the assumption $R_1\simeq R_2\simeq 2$. In order to get (E13) and (E14) to be of the form (4) and (5), we further take $l_{12}=l_{21}=2\alpha^*$ and obtain:

$$\dot{\theta}_1 = 1-\varepsilon\alpha^*\sin(\theta_1-\theta_2) \tag{E15}$$

$$\dot{\theta}_2 = 1+\varepsilon\alpha^*\sin(\theta_1-\theta_2). \tag{E16}$$

For the *2:1 case*, we similarly require

$$2(c_{212}+c_{221})=-(a_{212}+a_{221})$$

to eliminate the cos terms from Eqs. (E11) and (E12). The coefficients of $\dot{X}_1X_2$ and $X_1\dot{X}_2$ in g_2 are b_{212} and b_{221} respectively. For convenience we set $b_{221}=0$, and $b_{122}=4b_{212}=4\beta^*$ to obtain:

$$\dot{\theta}_1 = 2-\varepsilon\beta^*\sin(\theta_1-2\theta_2) \tag{E17}$$

$$\dot{\theta}_2 = 1+\varepsilon\beta^*\sin(\theta_1-2\theta_2). \tag{E18}$$

References

1. Cohen, A. H., Holmes, P. J., Rand, R. H.: The nature of the coupling between segmental oscillators of the lamprey spinal generator for locomotion: A mathematical model. J. Math. Biol. **13**, 345–369 (1982)
2. Ermentrout, G. B., Kopell, N.: Frequency plateaus in a chain of weakly coupled oscillators, I. SIAM J. Math. Anal. **15**, 215–237 (1984)
3. Cole, J. D.: Perturbation Methods in Applied Mathematics. Waltham: Blaisdell 1968
4. Denjoy, A.: Sur les courbes définies par les équations differentielles a la surface du tore. J. Math. **17** (IV), 333–375 (1932)
5. Glass, L., Mackey, M. C.: Pathological conditions resulting from instabilities in physiological control systems. Ann. N.Y. Acad. Sci. **316**, 214–235 (1979)
6. Guckenheimer, J., Holmes, P.: Nonlinear Oscillations, Dynamical Systems, and Bifurcations of Vector Fields. New York: Springer 1983
7. Guevara, M. R., Glass, L.: Phase locking, period doubling bifurcations, and chaos in a mathematical model of a periodically driven oscillator: A theory for the entrainment of biological oscillators and the generation of cardiac dysrhythmias. J. Math. Biol. **14**, 1–23 (1982)
8. Hoppensteadt, F. C., Keener, J. P.: Phase locking of biological clocks. J. Math. Biol. **15**, 339–349 (1982)
9. Keith, W. L.: Phase Locking and Entrainment in Two Coupled Limit Cycle Oscillators. Ph.D. Thesis, Cornell University, pp. 17–32, 1983
10. Rand, R. H.: Computer Algebra in Applied Mathematics: An Introduction to MACSYMA. Boston: Pitman 1984
11. Rand, R. H., Holmes, P. J.: Bifurcation of periodic motions in two weakly coupled van der Pol oscillators. Int. J. Nonlinear Mech. **3**, 387–399 (1980)

12. Rand, R. H., Storti, D. W., Upadhyaya, S. K., Cooke, J. R.: Dynamics of coupled stomatal oscillators. J. Math. Biol. **15**, 131–149 (1982)
13. van der Pol, B., van der Mark, J.: The heart beat considered as a relaxation oscillation and electrical model of the heart. Phil. Mag. **6**, 763–775 (1928)
14. Minorsky, N.: Nonlinear oscillations. New York: Kreiger 1974

Received January 27/April 14, 1984